Hydrol. Earth Syst. Sci. Discuss., https://doi.org/10.5194/hess-2018-251
Manuscript under review for journal Hydrol. Earth Syst. Sci.
Discussion started: 14 May 2018

Hydrology and Earth System Sciences
Open Access
Discussions

Projected Climate Change Impacts on Future Streamflow of the Yarlung Tsangpo-Brahmaputra River

Ran Xu[1], Hongchang Hu[1], Fuqiang Tian[1*], Chao Li[2], Mohd Yawar Ali Khan[1]

1. *Department of Hydraulic Engineering, Tsinghua University, Beijing 100084, China*
2. *Pacific Climate Impact Consortium, University of Victoria, Victoria, British Columbia, V8W 2Y2, Canada*

Corresponding Author: Fuqiang Tian (tianfq@tsinghua.edu.cn)

Hydrol. Earth Syst. Sci. Discuss., https://doi.org/10.5194/hess-2018-251
Manuscript under review for journal Hydrol. Earth Syst. Sci.
Discussion started: 14 May 2018

Hydrology and Earth System Sciences
Open Access
Discussions

Abstract

The Yarlung Tsangpo-Brahmaputra River (YBR) originating from the Tibetan Plateau (TP), is an important water source for many domestic and agricultural practices in countries including China, India, Bhutan and Bangladesh. To date, only a few studies have investigated the impacts of climate change on water resources in this river basin with dispersed results. In this study, we provide a comprehensive and updated assessment of the impacts of climate change on YBR streamflow by integrating a physically based hydrological model, regional climate integrations from CORDEX (Coordinated Regional Climate Downscaling Experiment), different bias correction methods, and Bayesian model averaging method. We find that (i) bias correction is able to reduce systematic biases in regional climate integrations and thus benefits hydrological simulations over YBR Basin; (ii) Bayesian model averaging, which optimally combines individual hydrological simulations obtained from different bias correction methods, tends to provide hydrological time series superior over individual ones. We show that by the year 2035, the annual mean streamflow is projected to change respectively by 6.8%, -0.4%, and -4.1% under RCP4.5 relative to the historical period (1980-2001) at the Bahadurabad in Bangladesh, the upper Brahmaputra outlet, and Nuxia in China. Under RCP8.5, these percentage changes will substantially increase to 12.9%, 13.1%, and 19.9%. Therefore, the change rate of streamflow shows strong spatial variability along the YBR from downstream to upstream. The increasing rate of streamflow shows an augmented trend from downstream to upstream under RCP8.5 compared to an attenuated pattern under RCP4.5.

Keywords: Climate Change Impacts, Yarlung Tsangpo-Brahmaputra River, Streamflow, Regional Climate Integrations, Bias Correction, Bayesian Model Averaging

Hydrol. Earth Syst. Sci. Discuss., https://doi.org/10.5194/hess-2018-251
Manuscript under review for journal Hydrol. Earth Syst. Sci.
Discussion started: 14 May 2018

Hydrology and Earth System Sciences
Discussions

1. Introduction

Water is a standout necessity amongst the most basic factors in human sustenance (Barnett et al., 2005). Global climate change has been found to intensify the global hydrological cycle, likely creating predominant impacts on regional water resources (Arnell, 1999; Gain et al., 2011). Evaluation of the potential impacts of anthropogenic climate change on regional and local water resources relies largely on climate model projections (Li et al., 2014). The spatial resolution of typical global climate models (GCMs) (100–300 km) is insufficient to simulate regional events that are needed to capture different climate and weather phenomena at regional to local scales (e.g., the watershed scale) (Olsson et al., 2015). Climate simulations from GCMs can be dynamically downscaled with regional climate models (RCMs) to scales of 25–50 km. Despite that dynamical downscaling is computationally very demanding and that its accuracy depends to a large extend on that of its parent GCM, dynamical downscaling can provide more detailed information on finer temporal and spatial scales than GCMs (Hewitson and Crane, 1996). Such information is valuable for impact projections at regional to local scales that are more relevant to water resources management.

On the other hand, although the increased horizontal resolution can improve the simulation of regional and local climate features, RCMs still produce biases in the time series of climatic variables (Christensen et al., 2008; Rauscher et al., 2010). Bias correction is typically applied to the output of climate models. Most bias correction methods correct variables separately, with interactions among variables typically not considered (Christensen et al., 2008; Hessami et al., 2008; Ines and Hansen, 2006; Johnson and Sharma, 2012; Li et al., 2010; Piani et al., 2009; Piani et al., 2010). Separate-variable bias correction methods, for example, may result in physically

55 unrealistic corrections (Thrasher et al., 2012) and do not correct errors in multivariate
56 relationships (Dosio and Paruolo, 2011). Correspondingly, Li et al. (2014) introduced a joint bias
57 correction (JBC) method and applied it to precipitation (P) and temperature (T) fields from the
58 fifth phase of the Climate Model Intercomparison Project (CMIP5) model ensemble.

59 The Yarlung Tsangpo-Brahmaputra River (YBR) is an important river system originating from
60 the Tibetan Plateau (TP), characterized by a dynamic fluvial regime with exceptional
61 physiographic setting spread along the eastern Himalayan region (Goswami, 1985). Critical
62 hydrological processes like snow and glacial melt are more important in this area compared to
63 others. Hydrological processes of the YBR Basin are highly sensitive to changes in temperature
64 and precipitation, which subsequently affect the melting characteristics of snowy and glaciered
65 areas and thus affect streamflow. The YBR Basin is also one of the most under-investigated and
66 underdeveloped basins around the world, with only few studies examined the impacts of climate
67 change on the hydrology and water resources of this basin (Immerzeel et al., 2010; Lutz et al.,
68 2014; Masood et al., 2015). Immerzeel et al. (2010) developed a snowmelt-runoff model in the
69 upper YBR Basin using native output (without bias correction) from 5 GCMs under the A1B
70 scenarios for 2046-2065 and found that its streamflow would decrease by 19.6% relative to
71 2000-2007. Subsequently, Lutz et al. (2014) implemented the SPHY (Spatial Processes in
72 Hydrology) hydrological model in the upper YBR Basin using native simulations from 4 GCMs
73 under RCP4.5 and RCP8.5 emissions scenarios for 2041-2050 and showed that the streamflow
74 would increase by 4.5% and 5.2% relative to 1998-2007 under the examined two emissions
75 scenarios. Masood et al. (2015) applied the H08 Hydrological model to the YBR Basin using
76 bias corrected projections of 5 GCMs for near future (2015-2039) and far future (2075-2099)

periods and found that relative to the period 1980-2001, the streamflow would increase by 6.7% and 16.2% for near and far future under RCP8.5, respectively.

Several factors could contribute to the discrepancy between these projections, such as the lack of high quality streamflow observations for hydrological model calibration, the choice of bias correction methods, simulations from global climate models, and future emissions scenarios, and a combination thereof. On the other hand, all the existing studies in the YBR basin rely on GCMs, which, as was discussed, cannot capture fine-scale climate and weather details that are required for a reliable regional impacts assessment. In the present study, we attempt to fill this gap by taking advantage of the recently compiled multi-model and multi-member high-resolution regional climate integrations from CORDEX (Coordinated Regional Climate Downscaling Experiment). We use different bias correction methods to alleviate the inherent biases in these regional climate integrations, and use a Bayesian model averaging technique to best combine different streamflow simulations obtained with different bias-corrected meteorological forcing data (e.g., precipitation and temperature). We synthesize our results and those in the existing studies with a hope to obtain a more comprehensive picture of changes in water resources in the YBR Basin in response to global climate warming.

We structured the paper into the following sections. Section 1 formulates the objectives of this study. Section 2 briefly introduces the YBR Basin, followed by the used materials and methods. Our results and those in existing studies are compared in Section 3. Main conclusions along with a brief discussion of the future scope of this study are presented in Section 4.

2. Materials and methodology

2.1 The Yarlung Tsangpo-Brahmaputra River Basin

Tibetan Plateau (TP) is often referred as Asia's water tower, bordered by India and Pakistan in the west side and Bhutan and Nepal on the southern side, with a mean elevation of about 4000 m above sea level (Tong et al., 2014). The YBR is one of the largest rivers originating from the TP in Southwest China at an elevation of about 3100 m above sea level (Goswami, 1985; Xu et al., 2017). The total length of the river is about 2900 km (Masood et al., 2015), with a drainage area of the basin estimated to be around 530,000 km^2. The YBR travels through China, Bhutan, and India before emptying into the Bay of Bengal in Bangladesh (Figure 1). The mean annual discharge is approximately 20,000m^3/s (Immerzeel, 2008). The climate of the basin is monsoon-driven with an obvious wet season from June to September, which accounts for 60–70% of the annual rainfall.

2.2 Data

2.2.1 Forcing data sets

Due to the lack of adequate in-situ meteorological observations, the WATCH forcing data (WFD) (Weedon et al., 2014) were used as a reference for bias correction and hydrological model calibration (Table 1). This dataset provided a good representation of real meteorological events and climate trends (Weedon et al., 2011). In this study, we used daily rainfall, temperature and potential evapotranspiration (*PET*) data from 1980 to 2001.

The sources of other required non-meteorological variables for implementing the hydrological model are as follows. The 90-m resolution digital elevation model data were acquired from the Shuttle Radar Topography Mission (SRTM) (http://srtm.csi.cgiar.org/). The Leaf Area Index (LAI) and snow cover data from 2000 to 2016 were downloaded from the National Aeronautics and Space Administration (NASA) (https://reverb.echo.nasa.gov/reverb/). For the periods during which LAI and snow data did not cover, average values of LAI and snow were used as model

input. The biweekly normalized difference vegetation index (NDVI) data from 1982 to 2000 with a spatial resolution of 8 km were obtained from the Global Inventory Modeling and Mapping Studies-Advanced Very High Resolution Radiometer (GIMMS-AVHRR) (http://www.glcf.umd.edu/data/gimms/). The soil hydraulic parameters were derived from the soil classification data which were extracted from the global digital soil map with a spatial resolution of 10 km (http://www.fao.org/geonetwork/).

2.2.2 Hydrological data

The streamflow observations during 1980-2001 for hydrological model calibration were obtained at two hydrological stations, i.e., the Nuxia station located in upstream China (Gao et al. (2008)) and the Bahadurabad station located in downstream Bangladesh; see Figure 1 for their geographical locations.

2.2.3 RCM data

The simulations of daily precipitation and temperature during the historical period of 1980-2001 and the projections under two examined emissions scenarios (RCP4.5 and RCP8.5) during the future period of 2020-2035 from the CORDEX experiment for the East Asia domain (which covers the whole YBR Basin) were downloaded from http://www.cordex.org/. The CORDEX program, which was coordinated by the World Climate Research Program, provides a unique opportunity for generating high-resolution regional climate projections and for assessing the impacts of future climate change at regional scales (Piani et al., 2009). As shown in Table 1, climate data from 5 CORDEX models were chosen. These models include HadGEM3-RA (denoted by RCM1), RegCM4 (RCM2), SNU-MM5 (RCM3), SNU-WRF (RCM4) and YSU-RSM (RCM5). To keep consistent with the WATCH forcing data, climate model integrations were interpolated to the grid of the WFD using the bilinear interpolation method.

Hydrol. Earth Syst. Sci. Discuss., https://doi.org/10.5194/hess-2018-251
Manuscript under review for journal Hydrol. Earth Syst. Sci.
Discussion started: 14 May 2018

The adopted hydrological model, as will be introduced later, also requires *PET* as a forcing variable. We used the method proposed by Leander and Buishand (2007) and S. C. van Pelt (2009) to calculate *PET* with daily temperature *T* as follows:

$$PET = [1 + \alpha_0 (T - \overline{T_0})] \overline{PET_0} \quad (1)$$

where $\overline{T_0}$ is the observed mean temperature (◦C) and $\overline{PET_0}$ is the observed mean PET_0 (mm/day) during the historical period. Daily PET_0 data were acquired directly from the WFD dataset and were used to compute $\overline{PET_0}$. The proportionality constant α_0 was determined for each calendar month by regressing the observed *PET* at each grid cell onto the observed daily temperature.

2.3 Methodology

2.3.1 Hydrological model: THREW

We adopted the Tsinghua Representative Elementary Watershed (THREW) model (Tian, 2006; Tian et al., 2006) to simulate streamflow of the YBR Basin. The model consists of a set of balance equations for mass, momentum, energy and entropy, including associated constitutive relationships for various exchange fluxes, at the scale of a well-defined spatial domain. Details of the model can be found in Tian et al. (2006). The THREW model has been successfully applied to quite a few watersheds across China and United States (Li et al., 2012; Mou et al., 2008; Sun et al., 2014; Tian et al., 2006; Tian et al., 2012; Xu et al., 2015; Yang et al., 2014). For the simulation of snow and glacier melting processes which is important for the YBR Basin, we modify the original THREW model by incorporating the temperature-index method introduced in Hock (2003). The index-temperature method has been shown to exhibit an overall good performance in mountain areas in China (He et al., 2015).

Hydrol. Earth Syst. Sci. Discuss., https://doi.org/10.5194/hess-2018-251
Manuscript under review for journal Hydrol. Earth Syst. Sci.
Discussion started: 14 May 2018

2.3.2 Bias correction methods

Quantile mapping (QM) with reference observations has been routinely applied to correct biases in RCM simulations (Maraun, 2013). Using WFD as reference observations and following the principle of QM, first we estimated cumulative distribution functions (CDFs) for the observed and native RCM-simulated time series of daily precipitation or temperature during the historical/calibration period (which is 1980-2001 in this study); then for a given RCM-simulated data value from an application period (which may be historical 1980-2001 period or future 2020-2035 period), we evaluated the CDF of the native RCM simulations at the given data value, followed by evaluation of the inverse of the CDF of the observations at the thus obtained CDF value; the resulting value is the bias-corrected simulation (see Figure 2 for an schematic illustration of this procedure).

Independent bias correction for multiple meteorological variables can produce non-physical corrections. To alleviate the deficits of independent bias correction, Li et al. (2014) introduced a joint bias correction (JBC) method, which takes the interactions between precipitation and temperature into account. This approach is based on a general bivariate distribution of P-T and essentially can be seen as a bivariate extension of the commonly used univariate QM method. Depending on the sequence of correction, there are two versions of JBC including JBCp, which corrects precipitation first and then temperature, and JBCt, which corrects temperature first and then precipitation. For more details of the QM and JBC methods, readers can refer to Wlicke et al. (2013) and Li et al. (2014), respectively.

2.3.3 Bayesian model averaging method

Bayesian model averaging (BMA) is a statistical technique designed to infer a prediction by weighted averaging predictions from different models/simulations. We refer readers to Dong et

Hydrol. Earth Syst. Sci. Discuss., https://doi.org/10.5194/hess-2018-251
Manuscript under review for journal Hydrol. Earth Syst. Sci.
Discussion started: 14 May 2018

189 al. (2013), which have presented a nice description of the basic principle of this method and the
190 Expectation-Maximization (EM) algorithm for optimally searching the BMA weights. Several
191 studies have applied BMA to RCMs or GCMs simulations to assess climate change impacts on
192 hydrology with meaningful results (Bhat et al., 2011; Duan et al., 2007; Wang and Robertson,
193 2011; Yang et al., 2011).

194 3. Results and discussion

195 3.1 Bias correction of meteorological variables during the historical period

196 We applied the three bias correction methods (i.e., QM, JBCp and JBCt) to the CORDEX
197 simulations of daily precipitation and temperature. We found that without bias correction, the
198 native RCM1 and RCM2 simulations (see Table 1 for the full names of different RCMs)
199 overestimate precipitation for all months during the 1980-2001 baseline period (Figure 3a-3b),
200 while native simulations by the other models tend to overestimate precipitation of the dry-season
201 (November to May of next year) and underestimate precipitation of other months. After bias
202 correction, the above mentioned overestimation and underestimation reduces considerably. For
203 temperature, we found that all the examined climate models consistently exhibit cold biases
204 across all the months, and that such biases are largely eliminated after applying bias correction
205 (Figure 4). In general, the three bias correction methods exhibit similar skills in reducing
206 temperature biases (Table 2), with JBCt and QM showing somewhat better performance than
207 JBCp. As expected, *PET* calculated from bias-corrected temperature simulations was quite close
208 to WFD observations.

209 In summary, we found that almost all the bias correction methods can substantially reduce biases
210 for all the three variables across the months, though with sizeable variations between bias

Hydrol. Earth Syst. Sci. Discuss., https://doi.org/10.5194/hess-2018-251
Manuscript under review for journal Hydrol. Earth Syst. Sci.
Discussion started: 14 May 2018

correction methods and across variables and seasons, consistent with existing studies on the comparison of different bias correction methods (Maraun, 2013; Prasanna, 2016).

3.2 Hydrological model setup and simulation

To setup the THREW model, the whole basin was discretized into 237 representative elementary watersheds (REWs). There are in total 16 parameters involved in THREW, as listed in Table 3. The first 6 parameters were determined for each REW a prior from the data described in the section 'Materials and methodology'. The remaining parameters were subjected to calibration and assumed to be uniform across the 237 REWs. Automatic calibration was implemented by the ε-NSGAII optimization algorithm developed by Reed et al. (2003). We chose the commonly used Nash Sutcliffe efficiency coefficient (NSE) (Nash and Sutcliffe, 1970) as the single objective function for model calibration.

We divided the whole period 1980-2001 into two sub-periods, which were used respectively for model calibration (1980-1990) and validation (1991-2001). Simulated daily streamflow time series at Bahadurabad were compared against the corresponding observations to compute the NSE objective function. To warm up the model, we dropped the first year of the calibration period (i.e., 1980). Observed and simulated daily streamflow of remaining years were used to compute NSE as follows:

$$\mathrm{NSE} = 1 - \frac{\sum_{n=1}^{N} (Q_o^n - Q_s^n)^2}{\sum_{n=1}^{N} (Q_o^n - \overline{Q_o})^2} \quad (2)$$

where N denotes the total number of days in the calibration period (which is 1981-1990 as one year is dropped for model warming up); Q_o^n and Q_s^n represent respectively the observed and simulated streamflow of day n; and $\overline{Q_o}$ is the average of observed streamflow during that period.

NSE is automatically optimized by the ε-NSGAII optimization algorithm. With the calibrated

232 model, NSE for the 1991-2001 validation period can be likewise computed so as to assess the
233 calibrated model performance in simulating streamflow that is not seen in the calibration period.

234 Figure 5 shows the observed (black line) and simulated (red line) discharges at Bahadurabad at
235 (a) daily, (b) monthly, and (c-d) seasonal time scales for both the calibration and validation
236 periods. It can be seen that the THREW model performs well in the YBR Basin at all time scales.
237 During the calibration period the daily and monthly NSE values are 0.84 and 0.92, respectively,
238 and during the validation period the daily and monthly NSE values are 0.78 and 0.84,
239 respectively. We also compared the observed and simulated monthly discharges at the Nuxia
240 station, which is not involved in model calibration. The monthly NSE values of calibration and
241 validation periods were 0.66 and 0.73, respectively. In summary, these results suggest that the
242 THREW model does a good job in simulating the hydrological processes in the YBR Basin
243 during this historical period. We assume that the calibrated THREW model is applicable to the
244 future period. This assumption is necessary in this study and has been widely adopted in previous
245 climate impacts studies.

246 Figure 6 compares the seasonal streamflow simulated by the THREW model with observed
247 streamflow data at Bahadurabad. It is observed that the streamflow generated by native RCM
248 simulations tends to either over- or underestimate the observations, and that all the adopted bias
249 correction methods can alleviate, to varying degrees, these biases. We found that in general bias
250 correction is more effective in improving the simulation of dry season streamflow (from
251 November to April in the next year) than that of wet season (May to October). Table 4 shows the
252 annual mean observed streamflow at Bahadurabad as well as the simulated streamflow with the
253 WFD data and with the native and bias-corrected RCM integrations. We can see that at annual
254 scale, streamflow simulated with native RCMs is on average higher (e.g., RCM1, RCM2) or

lower (e.g., RCM3, RCM4 and RCM5) than the observations; while streamflow simulated with bias-corrected RCMs is much more consistent with the observations.

Table 5 presents the NSE values for the daily and monthly streamflow over the calibration and validation periods simulated by the THREW model with the WFD data and with native and bias-corrected RCM simulations at Bahadurabad. We found that QM and JBCp can improve NSE for almost all the RCMs except RCM5, while JBCt can improve NSE for three of the five climate models (RCM1, RCM3, and RCM4). We also found that none of the 3 bias correction methods is compelling better than others, suggesting the necessity of combining different streamflow simulations generated with different bias-corrected climate simulations. Moreover, it is seen that most of the NSEs values are higher than 0.55 with a few exceptions, indicating reasonably well simulations of daily and monthly streamflow for both calibration and validation periods on average across the entire basin, and thus enhancing our confidence in applying the calibrated THREW model and the bias-corrected CORDEX simulations to projecting future hydrological conditions in the YBR Basin.

Given the fact that none of the bias correction methods and none of the RCM models are compellingly superior over others, as we have found, we therefore integrate streamflow simulations generated by different bias-corrected climate simulations from different climate models with different bias correction methods in terms of BMA. Our attempt is to take advantages of individual streamflow simulations. Daily streamflow simulations and observations during the THREW model calibration period (1981-1990) were used to calibrate the BMA weights, and those during the validation period are used to evaluate the calibrated BMA weights. In addition to NSE, two other indices were used to measure the closeness between observations

Hydrol. Earth Syst. Sci. Discuss., https://doi.org/10.5194/hess-2018-251
Manuscript under review for journal Hydrol. Earth Syst. Sci.
Discussion started: 14 May 2018

277 and simulations. These indices are relative error (RE) and root mean squared error (RMSE), both
278 evaluated at daily scale, as defined in the following:

$$\mathrm{RE} = 1 - \frac{\sum_{n=1}^{N} Q_s^n}{\sum_{n=1}^{N} Q_o^n} \quad (3)$$

$$\mathrm{RMSE} = \sqrt{\frac{\sum_{n=1}^{N}(Q_o^n - Q_s^n)^2}{N}} \quad (4)$$

279 where N denotes the total number of days during the considered period; Q_o^n and Q_s^n represent
280 respectively the observed and simulated streamflow of time n. As seen from Table 6, based on
281 the above indices, after applying BMA we obtain considerably better results than almost all those
282 generated by different bias-corrected climate simulations from different climate models with
283 different bias correction methods. Figure 7 shows the mean prediction (red line) and 90%
284 uncertainty interval of BMA during the historical period at Bahadurabad. The uncertainty
285 interval of BMA can cover almost all observations, which further indicated the sound
286 performance of BMA.

287 **3.3 Projections of future meteorological variables**

288 Figures 8-9 show changes in seasonal precipitation and temperature during the near future period
289 2020-2035 relative to the historical 1980-2001 period based on bias-corrected RCM simulations
290 under RCP4.5 and RCP8.5 emissions scenarios. It is found that precipitation in wet seasons will
291 increase under both emissions scenarios and in all bias-corrected RCM simulations with one
292 exception of RCM3 under RCP4.5. In contrast, precipitation in dry seasons is projected to
293 consistently decrease in all the studied RCM models. Therefore, the general pattern of "wet
294 getting wetter, dry getting drier" (Chou et al., 2013) associate with climate change exists in YBR
295 as well. Also, as expected, precipitation under RCP8.5 is on average higher than that under

296 RCP4.5, especially for RCM3 and RCM4 in the wet season. We also found obvious variations in
297 the projected changes among climate models and bias correction methods. This suggests the
298 importance of exploring multi-models and multi-methods to obtain a more comprehensive
299 picture about the uncertainty of the impacts of climate change on local hydrology. Using BMA
300 weight coefficient calculated in Section 3.2, weighted precipitation in historical period, RCP4.5
301 and RCP8.5 is 1425.3, 1529.8 and 1608.0 mm per year, respectively.

302 We found that temperature is projected to increase by all RCM simulations in both dry seasons
303 and wet seasons (Figure 9). It is surprising to see that there is no significant difference in
304 temperature between RCP8.5 and RCP4.5 scenarios except for RCM3 and RCM4. In fact, this is
305 not inconsistent with the IPCC AR5 (2013), which shows that the projected future global mean
306 temperature does not significantly diverge under different RCP scenarios until 2030 (our future
307 period is 2020-2035). Similar to precipitation, there are obvious variations in the projected
308 changes among different climate models and different bias correction methods. Using BMA
309 weight coefficient calculated in Section 3.2, weighted temperature in historical period, RCP4.5
310 and RCP8.5 is 8.7, 9.8 and 10.0℃, respectively.

311 **3.4 Projections of future streamflow and comparison with previous studies**

312 Figure 10 shows the mean prediction and 90% uncertainty interval of streamflow simulated by
313 BMA method during (a) RCP4.5, (b) RCP8.5 scenarios at Bahadurabad. Uncertainty interval of
314 RCP4.5 is similar with that of RCP8.5. All the following discussions in this subsection is based
315 on BMA weighted streamflow.

316 For the sake of comparison between Immerzeel et al. (2010), Lutz et al. (2014), Masood et al.
317 (2015) and our results, we also examined an upstream outlet location (the red dot in Figure 1),

318 which was studied in the referred studies. To be noted, the observed streamflow data at this
319 upstream outlet are unavailable.

320 Table 7 shows a summary of the referred existing studies about climate impact on future
321 streamflow in the YBR Basin. Immerzeel et al. (2010) developed Snowmelt Streamflow Model
322 for the upper YBR Basin using five GCMs in the A1B scenarios defined in IPCC AR4 during
323 2046-2065 without applying any bias correction methods or BMA method and the streamflow
324 will decrease by 19.6% when compared to the observed period (2000-2007). The SPHY model
325 developed by Lutz et al. (2014) for the upper YBR Basin using four GCMs in the RCP4.5 and
326 RCP8.5 scenarios during 2041-2050 and without applying any bias correction methods or BMA
327 method. The streamflow will increase by 4.5% and 5.2% in the RCP4.5 and RCP8.5 scenarios,
328 respectively when compared with the observed period (1998-2007). Masood et al. (2015) applied
329 H08 Hydrological model the YBR Basin using five GCMs during the near future (2015-2039)
330 and far future (2075-2099) and also applied bias correction method. The streamflow increased by
331 6.7% and 16.2% in the near future and far future, respectively, when compared with the observed
332 data (1980-2001).

333 The comparisons among the streamflow projection of YBR during different periods in different
334 studies are shown in Figure 11. In our study, the projected streamflow is 1466 mm/a during
335 2020-2035 under RCP8.5 at Bahadurabad, which is substantially higher than the findings of
336 Masood et al. (2015) at the same location, which is 1244 mm per year during 2015-2039 under
337 RCP8.5. The projected streamflow is 692 mm per year during 2020-2035 under RCP8.5 at the
338 upper YBR outlet. This result is quite close to the findings of Lutz et al. (2014), which is 727
339 mm per year during 2041-2050 under RCP8.5. To be noted, our study adopted RCMs
340 integrations, BMA method by incorporating different bias correction methods, and a physically

based hydrological model accounting for snow and glacier melting processes, which could explain the differences from the existing studies.

Table 8 shows the relative changes of projected runoff and its driving factors under different emission scenarios compared to the historical period at different locations of the YBR. At the basin-wide scale represented by Bahadurabad station, future streamflow shows an evidently increasing trend under both RCP4.5 and RCP8.5 scenarios. The increasing rate under RCP8.5 (12.9%) is not-surprisingly higher than RCP4.5 (6.8%). Also, the trends of streamflow exhibit strong spatial variability along the YBR. Under RCP4.5, upstream locations are more likely to experience an increasing trend at a much less rate. For example, the change rate of streamflow is projected to decrease at 0.4% and 4.1% at the YBR outlet and Nuxia, respectively. Under RCP8.5, however, upstream locations would more likely witness an augmented increasing rate of streamflow change, e.g., 13.1% and 19.9% at the YBR outlet and Nuxia, respectively.

4. Conclusions

In this study, we conducted a comprehensive evaluation of future streamflow in the YBR Basin. We adopted RCMs integrations, BMA method by incorporating different bias correction methods, and a physically based hydrological model accounting for snow and glacier melting processes to implement the evaluation. The major findings are summarized as follows.

(1) The three bias correction methods implemented in this study can all substantially reduce biases in the three variables (precipitation, temperature and potential evapotranspiration). Specifically for precipitation, when native RCMs show overestimations, all bias correction methods perform reasonably well. While, none of them can provide satisfying corrections when native RCMs exhibit strong underestimations. This finding is consistent with existing

363 studies (Maraun, 2013; Prasanna, 2016) and requires further in-deep studies. For
364 temperature and potential evapotranspiration, all of the three bias correction methods
365 performed well, especially QM and JBCt.

366 (2) The basin-wide discharge is projected to increase substantially during the future period
367 (2020-2035) under the two examined emissions scenarios of RCP4.5 and RCP8.5. The
368 projected annual mean streamflow at Bahadurabad is 1386.7 mm per year under RCP4.5
369 with an increasing rate of 6.9%, and the number becomes higher as 1466.4 mm per year
370 under RCP8.5 with an increasing rate of 12.9%. Increasing mean annual streamflow
371 indicates more flood events that would occur in this already vulnerable region, which calls
372 for more close collaborations among upstream and downstream riparian countries.

373 (3) Projected streamflow exhibits different spatial patterns under different scenarios in the YBR
374 basin. Under RCP4.5, the annual mean streamflow is projected to change by 6.8%, -0.4%,
375 and -4.1% in the future period (2020-2035) compared to the historical period (1980-2001) at
376 three locations from downstream to upstream along the YBR, i.e., Bahadurabad, the upper
377 YBR outlet, and Nuxia. Therefore, the increasing rate of streamflow exhibits an attenuated
378 trend from downstream to upstream. Under RCP8.5, however, the increasing rate of
379 streamflow (12.9%, 13.1%, and 19.9% at the three locations) exhibits an augmented trend
380 from downstream to upstream. The different trends are likely associated with varying spatial
381 patterns of projected future precipitation, but more detailed investigations are needed.

382

Hydrol. Earth Syst. Sci. Discuss., https://doi.org/10.5194/hess-2018-251
Manuscript under review for journal Hydrol. Earth Syst. Sci.
Discussion started: 14 May 2018

Acknowledgements

This study was financially supported by the National Science Foundation of China (91647205), the Ministry of Science and Technology of P.R. China (2016YFA0601603, 2016YFC0402701), and the foundation of State Key Laboratory of Hydroscience and Engineering of Tsinghua University (2016-KY-03).

Hydrol. Earth Syst. Sci. Discuss., https://doi.org/10.5194/hess-2018-251
Manuscript under review for journal Hydrol. Earth Syst. Sci.
Discussion started: 14 May 2018

References

Arnell, N. W.: Climate change and global water resources, Global Environ. Change, 9, 31-49, 1999.

Barnett, T. P., Adam, J. C., and Lettenmaier, D. P.: Potential impacts of a warming climate on water availability in snow-dominated regions, Nature, 438, 303-309, 2005.

Bhat, K. S., Haran, M., Terando, A., and Keller, K.: Climate Projections Using Bayesian Model Averaging and Space–Time Dependence, Journal of Agricultural, Biological, and Environmental Statistics, 16, 606-628, 2011.

Chou, C., Chiang, J. C. H., Lan, C.-W., Chung, C.-H., Liao, Y.-C., and Lee, C.-J.: Increase in the range between wet and dry season precipitation, Nature Geoscience, 6, 263-267, 2013.

Christensen, J. H., Boberg, F., Christensen, O. B., and LucasPicher, P.: On the need for bias correction of regional climate change projections of temperature and precipitation, 2008, Geophysical Research Letters, L20709, 2008.

Dong, L., Xiong, L., and Yu, K.-x.: Uncertainty Analysis of Multiple Hydrologic Models Using the Bayesian Model Averaging Method, Journal of Applied Mathematics, 2013, 1-11, 2013.

Dosio, A. and Paruolo, P.: Bias correction of the ENSEMBLES high-resolution climate change projections for use by impact models: Evaluation on the present climate, J. Geophys. Res., 116, 2011.

Duan, Q., Ajami, N. K., Gao, X., and Sorooshian, S.: Multi-model ensemble hydrologic prediction using Bayesian model averaging, Adv. Water Resour., 30, 1371-1386, 2007.

Gain, A. K., Immerzeel, W. W., Sperna Weiland, F. C., and Bierkens, M. F. P.: Impact of climate change on the stream flow of the lower Brahmaputra: trends in high and low flows based on discharge-weighted ensemble modelling, Hydrol. Earth Syst. Sci., 15, 1537-1545, 2011.

Gao, B., Yang, D., Liu, Z., and Zhu, C.: Application of a Distr ibuted Hydrological Model for the Yar lung Zangbo River and Analysis of the River Runoff, Journal of China Hydrology, 28, 40-44, 2008.

Goswami, D. C.: Brahmaputra River, Assam, India: Physiography, basin denudation, and channel aggradation, Water Resour. Res., 7, 959-978, 1985.

He, Z. H., Tian, F. Q., Gupta, H. V., Hu, H. C., and Hu, H. P.: Diagnostic calibration of a hydrological model in a mountain area by hydrograph partitioning, Hydrol. Earth Syst. Sci., 19, 1807-1826, 2015.

Hessami, M., Gachon, P., Ouarda, T. B. M. J., and St-Hilaire, A.: Automated regression-based statistical downscaling tool, Environmental Modelling & Software, 23, 813-834, 2008.

Hewitson, B. C. and Crane, R. G.: Climate downscaling: techniques and application, Clim. Res., 7, 85-95, 1996.

Hock, R.: Temperature index melt modelling in mountain areas, J. Hydrol., 282, 104-115, 2003.

Immerzeel, W. W.: Historical trends and future predictions of climate variability in the Brahmaputra basin, Int. J. Climatol., 28, 243-254, 2008.

Immerzeel, W. W., Van Beek, L. P., and Bierkens, M. F.: Climate change will affect the Asian water towers, Science, 328, 1382-1385, 2010.

Ines, A. V. M. and Hansen, J. W.: Bias correction of daily GCM rainfall for crop simulation studies, Agric. For. Meteorol., 138, 44-53, 2006.

Johnson, F. and Sharma, A.: A nesting model for bias correction of variability at multiple time scales in general circulation model precipitation simulations, Water Resour. Res., 48, 2012.

Leander, R. and Buishand, T. A.: Resampling of regional climate model output for the simulation of extreme river flows, J. Hydrol., 332, 487-496, 2007.

Li, C., Sinha, E., Horton, D. E., Diffenbaugh, N. S., and Michalak, A. M.: Joint bias correction of temperature and precipitation in climate model simulations, J. Geophys. Res. Atmos., 119, 153-162, 2014.

Li, H., Sheffield, J., and Wood, E. F.: Bias correction of monthly precipitation and temperature fields from Intergovernmental Panel on Climate Change AR4 models using equidistant quantile matching, J. Geophys. Res., 115, 2010.

Li, H., Sivapalan, M., and Tian, F.: Comparative diagnostic analysis of runoff generation processes in Oklahoma DMIP2 basins: The Blue River and the Illinois River, J. Hydrol., 418-419, 90-109, 2012.

Lutz, A. F., Immerzeel, W. W., Shrestha, A. B., and Bierkens, M. F. P.: Consistent increase in High Asia's runoff due to increasing glacier melt and precipitation, Nature Climate Change, 4, 587-592, 2014.

Maraun, D.: Bias Correction, Quantile Mapping, and Downscaling: Revisiting the Inflation Issue, J. Clim., 26, 2137-2143, 2013.

Masood, M., Yeh, P. J. F., Hanasaki, N., and Takeuchi, K.: Model study of the impacts of future climate change on the hydrology of Ganges–Brahmaputra–Meghna basin, Hydrol. Earth Syst. Sci., 19, 747-770, 2015.

Mou, L., Tian, F., Hu, H., and Sivapalan, M.: Extension of the Representative ElementaryWatershed approach for cold regions: constitutive relationships and an application, Hydrol. Earth Syst. Sci., 12, 565, 2008.

455 Nash, J. E. and Sutcliffe, J. V.: River flow forecasting through conceptual models Part I—A
456 discussion of principles, J. Hydrol., 10, 282-290, 1970.

457 Olsson, T., Jakkila, J., Veijalainen, N., Backman, L., Kaurola, J., and Vehvilä inen, B.: Impacts of
458 climate change on temperature, precipitation and hydrology in Finland – studies using bias
459 corrected Regional Climate Model data, Hydrol. Earth Syst. Sci., 19, 3217-3238, 2015.

460 Piani, C., Haerter, J. O., and Coppola, E.: Statistical bias correction for daily precipitation in
461 regional climate models over Europe, Theor. Appl. Climatol., 99, 187-192, 2009.

462 Piani, C., Weedon, G. P., Best, M., Gomes, S. M., Viterbo, P., Hagemann, S., and Haerter, J. O.:
463 Statistical bias correction of global simulated daily precipitation and temperature for the
464 application of hydrological models, J. Hydrol., 395, 199-215, 2010.

465 Prasanna, V.: Statistical bias correction method applied on CMIP5 datasets over the Indian
466 region during the summer monsoon season for climate change applications, Theor. Appl.
467 Climatol., doi: 10.1007/s00704-016-1974-8, 2016. 2016.

468 Rauscher, S. A., Coppola, E., Piani, C., and Giorgi, F.: Resolution effects on regional climate
469 model simulations of seasonal precipitation over Europe, Clim. Dyn., 35, 685-711, 2010.

470 Reed, P., Minsker, B. S., and Goldberg, D. E.: Simplifying multiobjective optimization: An
471 automated design methodology for the nondominated sorted genetic algorithm-II, Water Resour.
472 Res., 39, 2003.

473 S. C. van Pelt, P. K., H.W. ter Maat, B. J. J. M. van den Hurk, and A. H.Weerts: Discharge
474 simulations performed with a hydrological model using bias corrected regional climate model
475 input, Hydrol. Earth Syst. Sci., 13, 2387-2397, 2009.

476 Sun, Y., Tian, F., Yang, L., and Hu, H.: Exploring the spatial variability of contributions from
477 climate variation and change in catchment properties to streamflow decrease in a mesoscale
478 basin by three different methods, J. Hydrol., 508, 170-180, 2014.

479 Thrasher, B., Maurer, E. P., McKellar, C., and Duffy, P. B.: Technical Note: Bias correcting
480 climate model simulated daily temperature extremes with quantile mapping, Hydrol. Earth Syst.
481 Sci., 16, 3309-3314, 2012.

482 Tian, F.: Study on Thermodynamic Watershed Hydrological Model (THModel), Ph.D. Thesis,
483 2006. Department of Hydraulic Engineering, Tsinghua University, Beijing, China, 168 pp., 2006.

484 Tian, F., Hu, H., Lei, Z., and Sivapalan, M.: Extension of the Representative
485 ElementaryWatershed approach for cold regions via explicit treatment of energy related
486 processes, Hydrol. Earth Syst. Sci., 10, 619-644, 2006.

487 Tian, F., Li, H., and Sivapalan, M.: Model diagnostic analysis of seasonal switching of runoff
488 generation mechanisms in the Blue River basin, Oklahoma, J. Hydrol., 418-419, 136-149, 2012.

489 Tong, K., Su, F., Yang, D., Zhang, L., and Hao, Z.: Tibetan Plateau precipitation as depicted by
490 gauge observations, reanalyses and satellite retrievals, Int. J. Climatol., 34, 265-285, 2014.

491 Wang, Q. J. and Robertson, D. E.: Multisite probabilistic forecasting of seasonal flows for
492 streams with zero value occurrences, Water Resour. Res., 47, 2011.

493 Weedon, G. P., Balsamo, G., Bellouin, N., Gomes, S., Best, M. J., and Viterbo, P.: The WFDEI
494 meteorological forcing data set: WATCH Forcing Data methodology applied to ERA-Interim
495 reanalysis data, Water Resour. Res., 50, 7505-7514, 2014.

496 Weedon, G. P., Gomes, S., Viterbo, P., Shuttleworth, W. J., Blyth, E., Österle, H., Adam, J. C.,
497 Bellouin, N., Boucher, O., and Best, M.: Creation of the WATCH Forcing Data and Its Use to
498 Assess Global and Regional Reference Crop Evaporation over Land during the Twentieth
499 Century, J. Hydrometeorol., 12, 823-848, 2011.

500 Wlicke, R. A. I., Mendlik, T., and Gobiet, A.: Multi-variable error correction of regional climate
501 models, Climate Change, 120, 871-887, 2013.

502 Xu, R., Tian, F., Yang, L., Hu, H., Lu, H., and Hou, A.: Ground validation of GPM IMERG and
503 TRMM 3B42V7 rainfall products over southern Tibetan Plateau based on a high-density rain
504 gauge network, J. Geophys. Res. Atmos., 122, 910-924, 2017.

505 Xu, R., Tie, Q., Dai, C., Hu, H., and Tian, F.: Study on hydrological process in upper basin of
506 Brahmaputra River from Nuxia Hydrological Station and its response to climate change (in
507 Chinese), Journal of Hohai University (Natural Sciences), 43, 288-293, 2015.

508 Yang, H., Wang, B., and Wang, B.: Reducing biases in regional climate downscaling by
509 applying Bayesian model averaging on large-scale forcing, Clim. Dyn., 39, 2523-2532, 2011.

510 Yang, L., Tian, F., Sun, Y., Yuan, X., and Hu, H.: Attribution of hydrologic forecast uncertainty
511 within scalable forecast windows, Hydrol. Earth Syst. Sci., 18, 775-786, 2014.

512

513

Hydrol. Earth Syst. Sci. Discuss., https://doi.org/10.5194/hess-2018-251
Manuscript under review for journal Hydrol. Earth Syst. Sci.
Discussion started: 14 May 2018

List of Tables

Hydrol. Earth Syst. Sci. Discuss., https://doi.org/10.5194/hess-2018-251
Manuscript under review for journal Hydrol. Earth Syst. Sci.
Discussion started: 14 May 2018

Hydrology and Earth System Sciences
Discussions

531 Table 1. Description of the WATCH forcing data and 5 RCM datasets.

Type	Dataset	Spatial resolution	Temporal resolution	Period	Description
Observation data	WATCH Forcing Data (WFD)	0.5°	Daily	1980-2001	Rainfall, air temperature, potential evapotranspiration
RCM data	HadGEM3-RA (RCM1) RegCM (RCM2) SNU-MM5 (RCM3) SNU-WRF (RCM4) YSU-RSM (RCM5)	0.44°	Daily	1980-2001 2020-2035 (RCP4.5, RCP8.5)	Rainfall, air temperature, surface pressure, specific humidity

532
533

Hydrol. Earth Syst. Sci. Discuss., https://doi.org/10.5194/hess-2018-251
Manuscript under review for journal Hydrol. Earth Syst. Sci.
Discussion started: 14 May 2018

534 Table 2. Annual mean values of basin-wide precipitation (ppt), temperature (tmp) and potential
535 evapotranspiration (pet) calculated from WFD and native/corrected RCMs datasets.

		native	JBCp	JBCt	QM
ppt	WFD	1310			
mm /yr	RCM1	2025	1296	1283	1296
	RCM2	1834	1312	1299	1312
	RCM3	1101	1584	1726	1584
	RCM4	1242	1523	1617	1523
	RCM5	1381	1325	1338	1325
tmp	WFD	8.77			
℃	RCM1	5.80	8.85	8.77	8.77
	RCM2	4.48	8.69	8.77	8.77
	RCM3	4.99	8.23	8.77	8.77
	RCM4	3.77	8.57	8.77	8.77
	RCM5	0.36	8.38	8.77	8.77
pet	WFD	532			
mm /yr	RCM1	448	525	542	542
	RCM2	430	528	542	542
	RCM3	474	526	553	553
	RCM4	479	540	543	543
	RCM5	478	513	532	532

536
537

Hydrol. Earth Syst. Sci. Discuss., https://doi.org/10.5194/hess-2018-251
Manuscript under review for journal Hydrol. Earth Syst. Sci.
Discussion started: 14 May 2018

Hydrology and Earth System Sciences
Discussions

538 Table 3. Principal parameters of THREW model.

Symbol	Unit	Physical meaning	Range	Calibrated value
K_s^u	m/s	Saturated hydraulic conductivity for u-zone which is different for each REW. The value showing here is the averaged value over the whole catchment	-	6.25e-6
K_s^s	m/s	Similar to K_s^u, saturated hydraulic conductivity for s-zone	-	6.25e-6
ε^u	-	Soil porosity value of u-zone which is different for each REW. The value showing here is averaged over the whole catchment	-	0.47
ε^s	-	Similar to ε^u, soil porosity of s-zone	-	0.28
ψ_a	m	Air entry value which is different for each REW. The value showing here is averaged over the whole catchment	-	0.25
μ	-	Soil pore size distribution index in $\overline{f_e} = \alpha^{EFL} \frac{\overline{K_s^u}}{(1-s^u)y^u} \frac{(S^u)^{2+d}\varepsilon^u\lvert\psi_a\rvert}{\mu}$, where $\overline{f_e}$ is the exfiltration capacity from u-zone, s^u is the saturation degree of u-zone, y^u is the soil depth of u-zone, d is the diffusion index $(d=1+1/\mu)$. The value showing here is the averaged value over the whole catchment	-	0.20
n^t	-	Manning roughness coefficient for hillslope	0.005-1	0.03
n^r	-	Similar to n^r, Manning roughness coefficient for channel	0.005-1	0.006
B	-	Shape coefficient to calculate the saturation excess streamflow area	0.1-1	0.5
KKA	-	Coefficient to calculate subsurface flow in $R_g = KKD \cdot S \cdot K_S^S \cdot (y^S/Z)^{KKA}$, When S is the topographic slope, y^s is the depth of s-zone, Z is the total soil depth	1-30	5.0
KKD	-	See describe for *KKA*	0.1-1	0.5
α^{IFL}	-	Spatial heterogeneous coefficient for infiltration capacity	0.1-5	1.5
α^{EFL}	-	Spatial heterogeneous coefficient for exfiltration capacity	0.1-20	0.7
α^{ETL}	-	Spatial heterogeneous coefficient for evapotranspiration capacity	0.1-5	0.7
$DDFg$	mm℃day^{-1}	Degree day factor glacier	0-15	6.0
$DDFs$	mm℃day^{-1}	Degree day factor snow	0-15	4.8

539

540

Hydrol. Earth Syst. Sci. Discuss., https://doi.org/10.5194/hess-2018-251
Manuscript under review for journal Hydrol. Earth Syst. Sci.
Discussion started: 14 May 2018

Hydrology and Earth System Sciences
Discussions

Table 4. Annual mean observed discharge and simulated discharge forced by WFD and native/corrected RCMs datasets at the Bahadurabad station.

Discharge	Calibration period				Validation period			
$10^4 m^3/s$	native	QM	JBCp	JBCt	native	QM	JBCp	JBCt
obs	2.23				2.29			
WFD	2.08				2.09			
RCM1	3.12	2.01	2.07	1.97	3.23	2.11	2.16	2.07
RCM2	2.73	2.03	2.05	2.00	2.85	2.12	2.15	2.09
RCM3	1.80	2.34	2.31	2.55	1.84	2.37	2.33	2.61
RCM4	1.88	2.24	2.25	2.41	1.92	2.27	2.28	2.45
RCM5	2.02	1.87	1.89	1.90	2.24	2.08	2.10	2.13

Hydrol. Earth Syst. Sci. Discuss., https://doi.org/10.5194/hess-2018-251
Manuscript under review for journal Hydrol. Earth Syst. Sci.
Discussion started: 14 May 2018

Hydrology and Earth System Sciences
Discussions

546 Table 5. Nash-Sutcliffe efficiency coefficient (NSE) of streamflow simulation forced by WFD and native/corrected RCMs datasets at daily and
547 monthly time scales (denoted as day and mon in the table).

NSE	RCM1				RCM2				RCM3				RCM4				RCM5			
	calibration		validation		calibration		validation		calibration		validation		calibration		validation		calibration		validation	
	day	mon	day	mon	day	mon	day	mon	day	mon	day	mon	day	mon	day	mon	day	mon	day	mon
WFD	0.84	0.92	0.78	0.84																
RCM	-0.1	0.10	-0.0	0.17	0.46	0.61	0.39	0.51	0.52	0.64	0.40	0.53	0.56	0.70	0.56	0.67	0.56	0.69	0.54	0.70
RCM_QM	0.53	0.66	0.56	0.66	0.51	0.63	0.47	0.57	0.57	0.69	0.44	0.58	0.56	0.72	0.58	0.70	0.41	0.51	0.51	0.63
RCM_JBCp	0.56	0.69	0.58	0.69	0.53	0.66	0.49	0.60	0.58	0.71	0.46	0.60	0.57	0.72	0.59	0.70	0.42	0.52	0.51	0.63
RCM_JBCt	0.44	0.56	0.50	0.60	0.39	0.50	0.35	0.43	0.59	0.72	0.51	0.65	0.60	0.76	0.64	0.75	0.49	0.59	0.56	0.69

548

Hydrol. Earth Syst. Sci. Discuss., https://doi.org/10.5194/hess-2018-251
Manuscript under review for journal Hydrol. Earth Syst. Sci.
Discussion started: 14 May 2018

Hydrology and Earth System Sciences
Discussions

549 Table 6. Evaluation merits of streamflow simulations for individual RCM and BMA scenarios.

Scenarios		Calibration			Validation		
		NSE	RE (%)	RMSE (m^3/s)	NSE	RE (%)	RMSE (m^3/s)
QM	RCM1	0.53	9.9	12070.7	0.56	7.8	12519.3
	RCM2	0.51	9.0	12312.7	0.47	7.1	13701.0
	RCM3	0.57	-4.9	11573.7	0.44	-3.8	14158.6
	RCM4	0.56	-0.5	11633.8	0.58	0.5	12174.1
	RCM5	0.41	16.3	13487.3	0.51	8.9	13269.3
JBCp	RCM1	0.56	7.2	11703.5	0.58	5.4	12244.0
	RCM2	0.53	8.1	12061.4	0.49	6.0	13424.4
	RCM3	0.58	-3.4	11369.7	0.46	-1.9	13898.5
	RCM4	0.57	-0.9	11568.2	0.59	0.3	12134.9
	RCM5	0.42	15.4	13427.7	0.50	8.1	13264.3
JBCt	RCM1	0.44	11.9	13111.4	0.50	9.4	13374.6
	RCM2	0.39	10.5	13732.9	0.35	8.5	15243.1
	RCM3	0.59	-15.0	11204.6	0.51	-14.1	13165.9
	RCM4	0.60	-7.9	11161.9	0.64	-7.4	11347.8
	RCM5	0.49	15.0	12613.0	0.62	6.9	12564.8
BMA		0.64	6.9	10524.2	0.61	4.8	11745.9

Hydrol. Earth Syst. Sci. Discuss., https://doi.org/10.5194/hess-2018-251
Manuscript under review for journal Hydrol. Earth Syst. Sci.
Discussion started: 14 May 2018

Hydrology and Earth System Sciences
Discussions

Table 7. Summary of existing studies on projected streamflow under climate change in the YBR Basin.

Hydrological model	Study Area, Calibration Hydrological Station	GCMs/RCMs	Scenarios	Bias Correction	Bayesian Model Averaging	Streamflow Change Results	Reference
Snowmelt Runoff Model	upper YBR Basin, no calibration station	GCMs (CCMA-CGCM3, GFDL-CM2,MPIM-ECHAM5,NIES-MIROC3, UKMO-HADGEM1)	Obs (2000-2007) A1B (2046-2065)	No	No	-19.6%	Immerzeel et al. (2010)
Spatial Processes in Hydrology (SPHY) model	upper YBR Basin, no calibration station	GCMs (RCP4.5:GISS-E2-R, IPSL-CM5A-LR, CCSM4, CanESM2; RCP8.5: GFDL-ESM2G, IPSL-CM5A-LR, CSIRO-Mk3-6-0, CanESM2)	Obs (1998-2007) RCP4.5 (2041-2050) RCP8.5 (2041-2050)	No	No	4.5%(RCP4.5) 5.2%(RCP8.5)	Lutz et al. (2014)
H08 Hydrological model	YBR Basin, Bahadurabad	GCMs (MRI-AGCM3.2S, MIROC5, MIROC-ESM, MRI-CGCM3, HadGEM2-ES)	Obs (1980-2001) Near-future (2015-2039) Far-future (2075-2099)	Yes	No	6.7%(near-future) 16.2%(far-future) RCP8.5	Masood et al. (2015)
Tsinghua Representative Elementary Watershed (THREW) model	YBR Basin, Bahadurabad	RCMs(HadGEM3-RA, RegCM, SNU-MM5, SNU-WRF, YSU-RSM)	Obs (1980-2001) RCP4.5 (2006-2035) RCP8.5 (2006-2035)	Yes	Yes	6.8%(RCP4.5) 12.9%(RCP8.5)	This study

Hydrol. Earth Syst. Sci. Discuss., https://doi.org/10.5194/hess-2018-251
Manuscript under review for journal Hydrol. Earth Syst. Sci.
Discussion started: 14 May 2018

Hydrology and Earth System Sciences
Discussions

553 Table 8. Means of precipitation / temperature / runoff in the future period (2020-2035) and their relative changes compared to the historical period
554 (1980-2001) under different scenarios in the YRB.

	P (mm/a)	R_P **(%)**	**T (℃)**	R_T **(℃)**	**R (mm/a)**	R_R **(%)**	r_R	r_G	r_S
His-B	1425.3	-	8.7	-	1298.4	-	87.0%	3.2%	97%
fs4.5-B	1529.8	7.3%	9.8	1.1	1386.7	6.8%	86.5%	3.3%	10.2%
fs8.5-B	1608.0	12.8%	10.0	1.3	1466.4	12.9%	86.9%	3.2%	10.0%
His-O	668.9	-	1.0	-	611.6	-	68.9%	9.0%	22.1%
fs4.5-O	639.9	-4.4%	2.2	1.3	609.3	-0.4%	64.4%	9.9%	25.7%
fs8.5-O	748.3	11.9%	2.6	1.6	691.9	13.1%	67.4%	9.0%	23.6%
His-N	631.6	-	-0.1	-	485.8	-	74.4%	5.3%	20.3%
fs4.5-N	595.8	-5.7%	1.2	1.3	465.8	-4.1%	69.3%	6.1%	24.6%
fs8.5-N	712.0	12.7%	1.6	1.7	582.5	19.9%	74.8%	5.0%	20.3%

555 Note: P denotes precipitation, T denotes temperature, R denotes runoff; R_P, R_T, R_R denote relative changes of P, T and R compared to
556 the historical period, respectively; r_R, r_G, r_S denotes the ratio of rainfall, glacier melting, and snow melting induced runoff in the total
557 runoff, respectively; -B denotes Bahadurabad, -O denotes he upper YBR basin outlet, and -N denotes Nuxia.
558

Hydrol. Earth Syst. Sci. Discuss., https://doi.org/10.5194/hess-2018-251
Manuscript under review for journal Hydrol. Earth Syst. Sci.
Discussion started: 14 May 2018

Hydrology and Earth System Sciences
Discussions

List of Figures

Hydrol. Earth Syst. Sci. Discuss., https://doi.org/10.5194/hess-2018-251
Manuscript under review for journal Hydrol. Earth Syst. Sci.
Discussion started: 14 May 2018

Hydrology and Earth System Sciences
Discussions

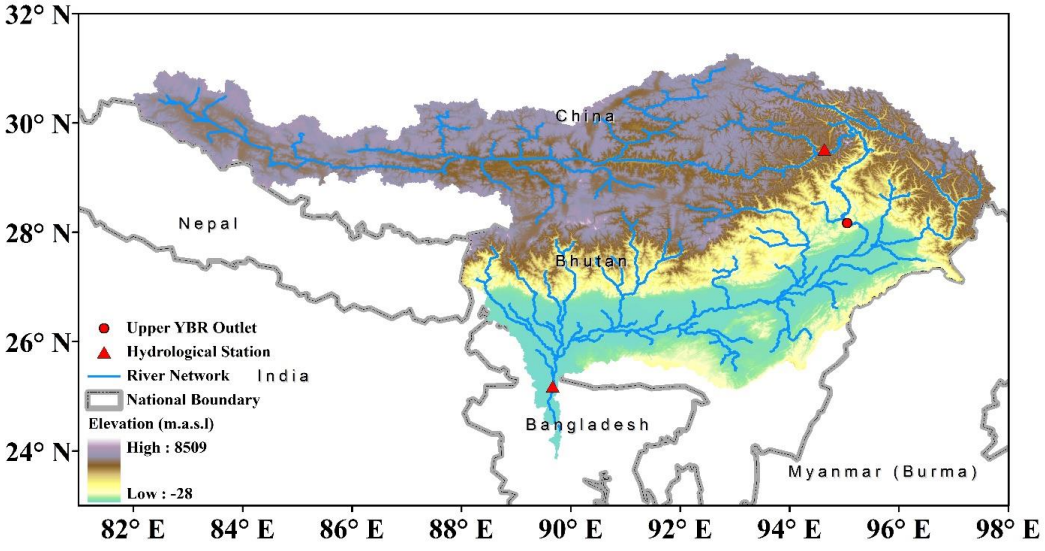

589

590 Figure 1. Study area, river network and location of hydrological stations (Nuxia in the upstream basin,

591 Bahadurabad in the downstream basin).

Hydrol. Earth Syst. Sci. Discuss., https://doi.org/10.5194/hess-2018-251
Manuscript under review for journal Hydrol. Earth Syst. Sci.
Discussion started: 14 May 2018

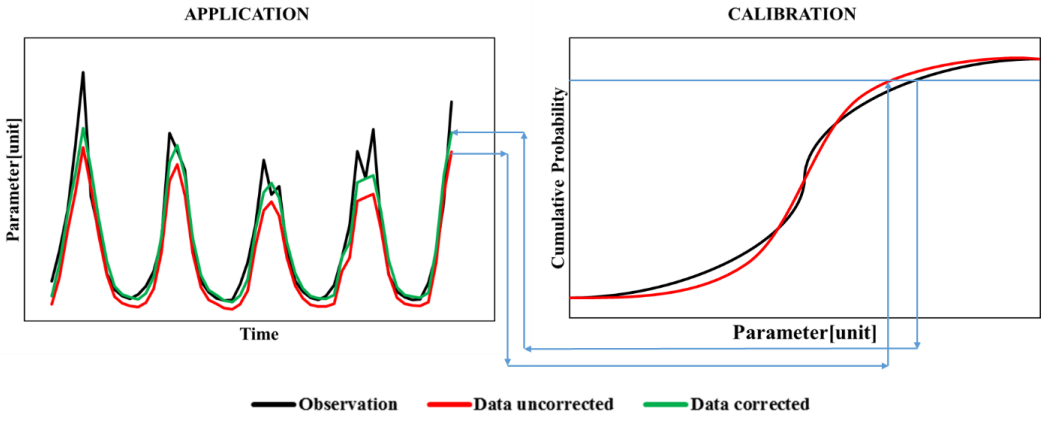

592

593 Figure 2. Schematic illustration of quantile mapping bias correction method applied in the paper (Wlicke

594 et al., 2013).

595

Hydrol. Earth Syst. Sci. Discuss., https://doi.org/10.5194/hess-2018-251
Manuscript under review for journal Hydrol. Earth Syst. Sci.
Discussion started: 14 May 2018

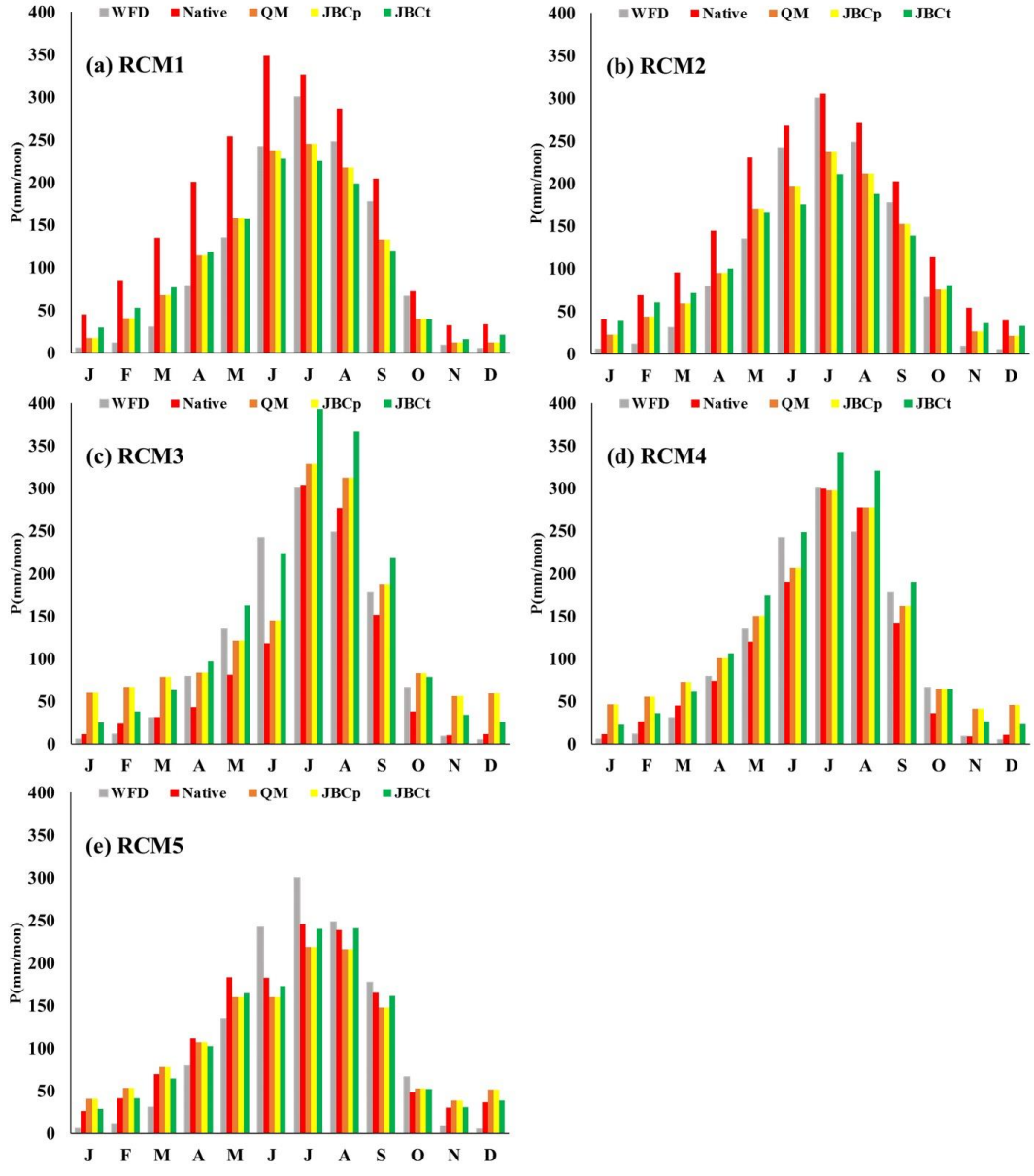

596

597 Figure 3. Seasonal cycles of precipitation from WFD and native/corrected RCMs during the historical

598 period (1980-2001). (a) for RCM1, (b) for RCM2, (c) for RCM3, (d) for RCM4, (e) for RCM5.

599

Hydrol. Earth Syst. Sci. Discuss., https://doi.org/10.5194/hess-2018-251
Manuscript under review for journal Hydrol. Earth Syst. Sci.
Discussion started: 14 May 2018

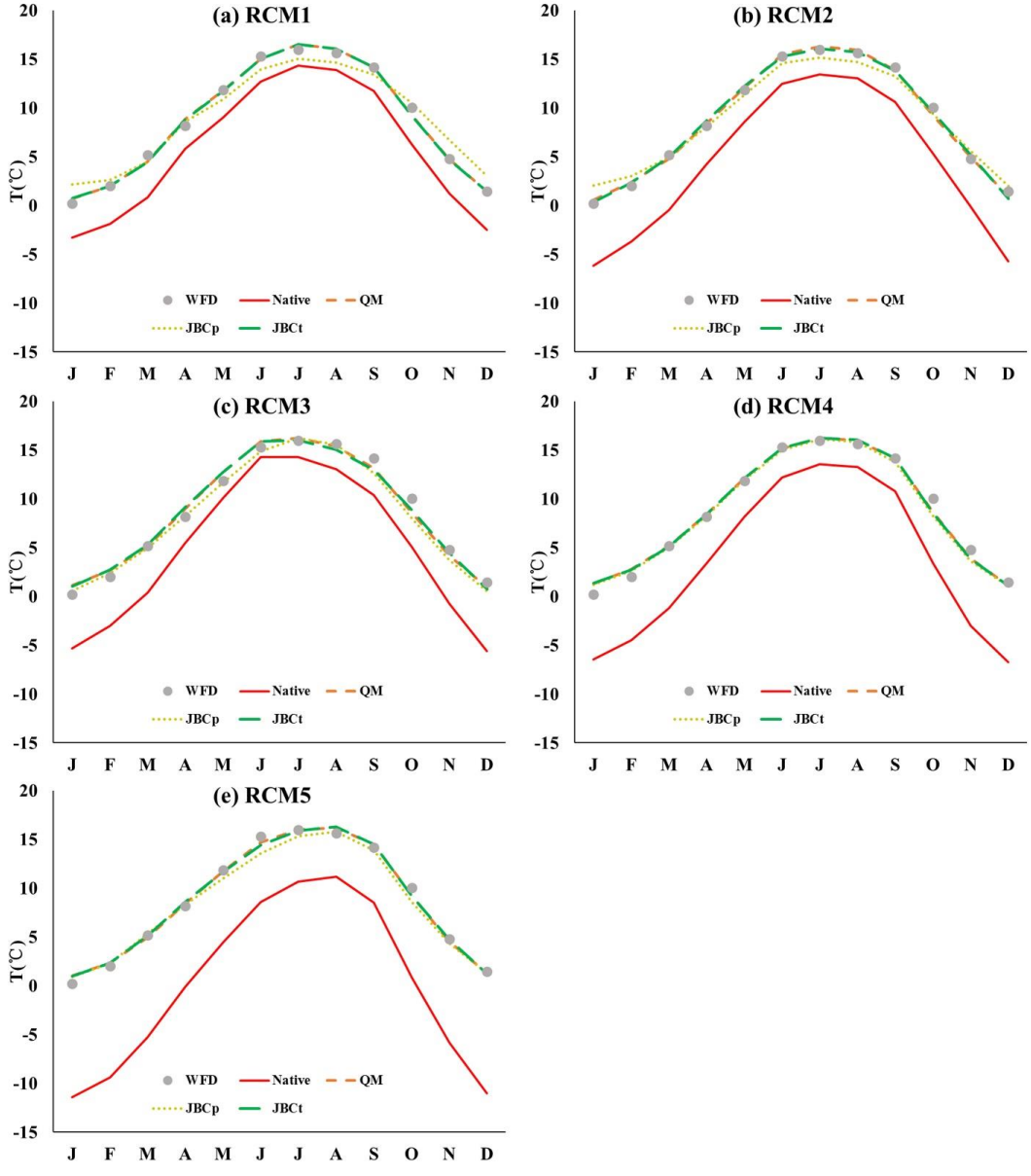

Figure 4. Seasonal cycles of temperature from WFD and native/corrected RCMs during the historical period (1980-2001). (a) for RCM1, (b) for RCM2, (c) for RCM3, (d) for RCM4, (e) for RCM5.

Hydrol. Earth Syst. Sci. Discuss., https://doi.org/10.5194/hess-2018-251
Manuscript under review for journal Hydrol. Earth Syst. Sci.
Discussion started: 14 May 2018

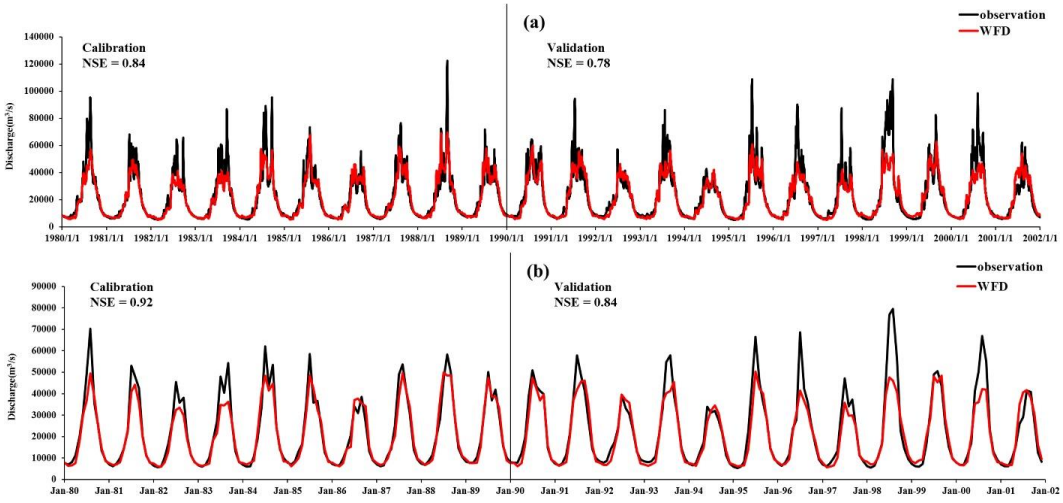

Figure 5. The simulated (red line) and observed (black line) discharge at Bahadurabad at the (a) daily scale, (b) monthly scale.

Hydrol. Earth Syst. Sci. Discuss., https://doi.org/10.5194/hess-2018-251
Manuscript under review for journal Hydrol. Earth Syst. Sci.
Discussion started: 14 May 2018

Hydrology and Earth System Sciences
Discussions

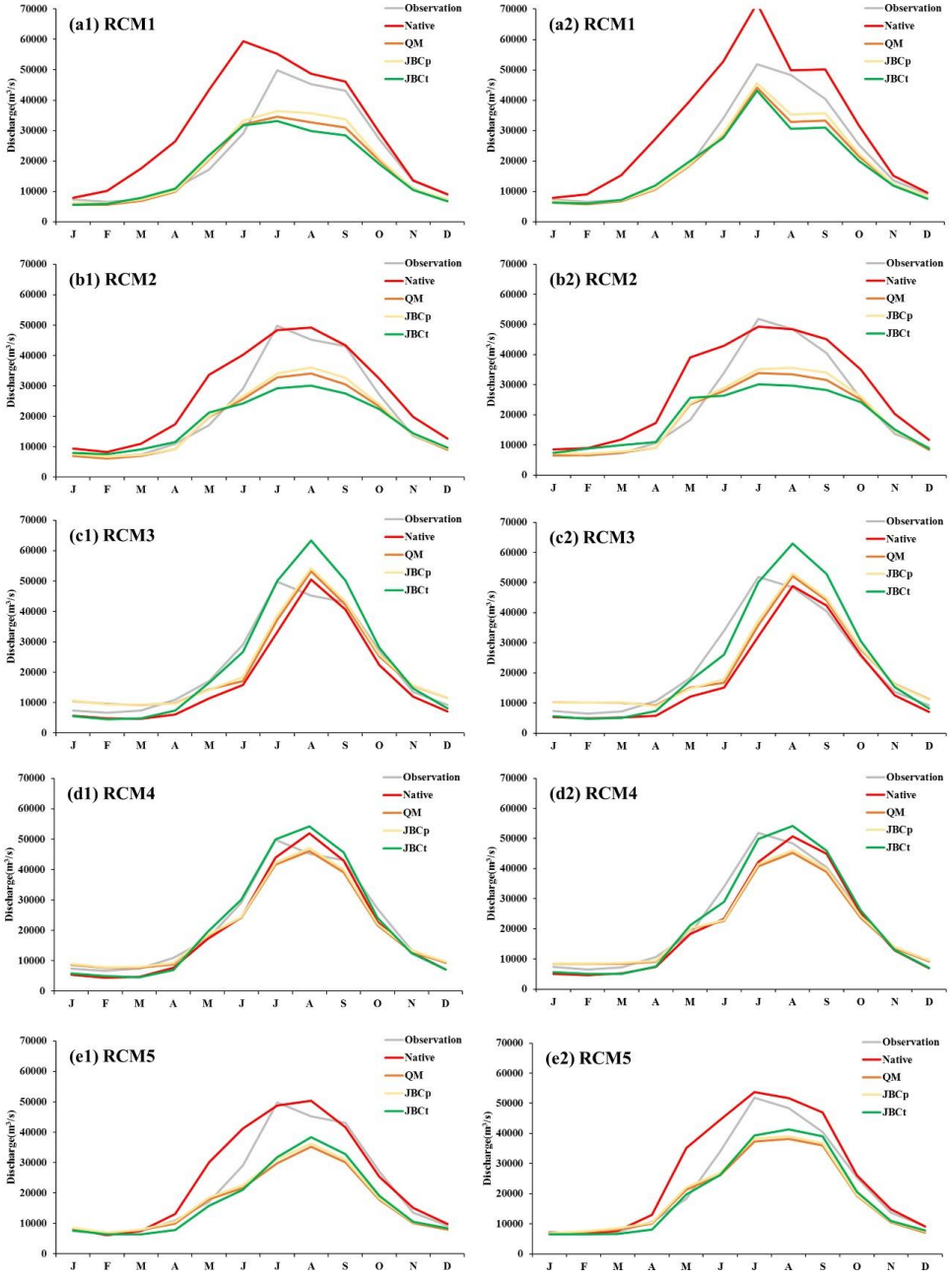

608
609 Figure 6. Seasonal cycles of observed streamflow and simulated streamflow forced by WFD and
610 native/corrected RCMs during the calibration period (left column) and validation period (right column) at
611 Bahadurabad.

Hydrol. Earth Syst. Sci. Discuss., https://doi.org/10.5194/hess-2018-251
Manuscript under review for journal Hydrol. Earth Syst. Sci.
Discussion started: 14 May 2018

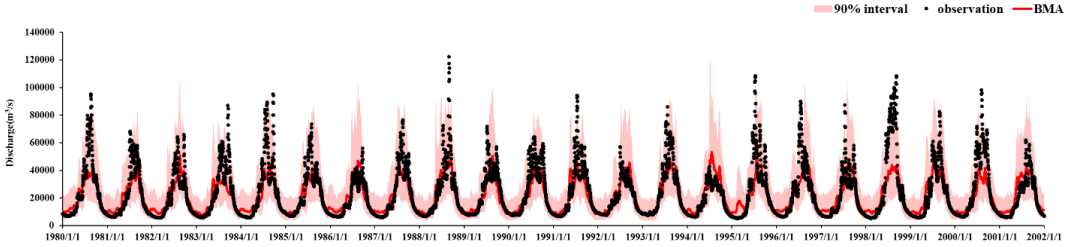

Figure 7. The mean values and 90% uncertainty interval of streamflow simulated by the BMA method during the historical period.

Hydrol. Earth Syst. Sci. Discuss., https://doi.org/10.5194/hess-2018-251
Manuscript under review for journal Hydrol. Earth Syst. Sci.
Discussion started: 14 May 2018

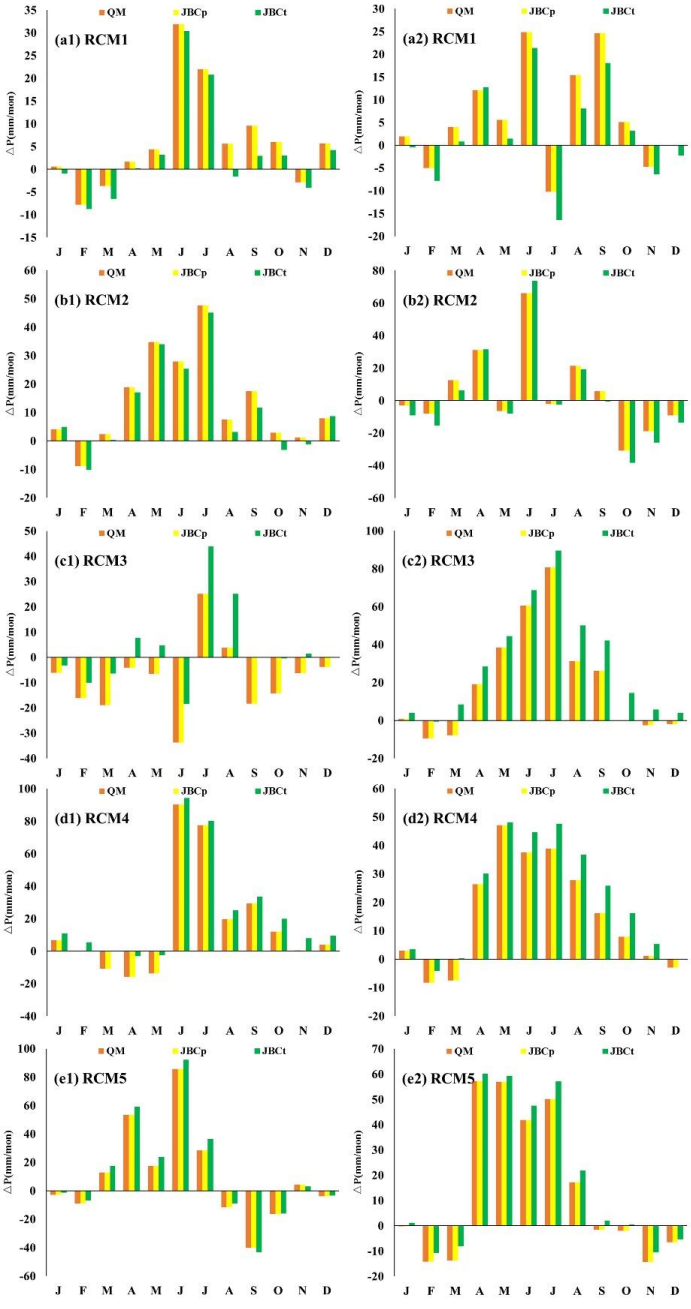

Figure 8. Change of basin-wide precipitation in the future period projected by corrected RCMs under RCP4.5 (left column) and RCP8.5 (right column) scenarios compared to the historical period.

Hydrol. Earth Syst. Sci. Discuss., https://doi.org/10.5194/hess-2018-251
Manuscript under review for journal Hydrol. Earth Syst. Sci.
Discussion started: 14 May 2018

Hydrology and Earth System Sciences
Discussions

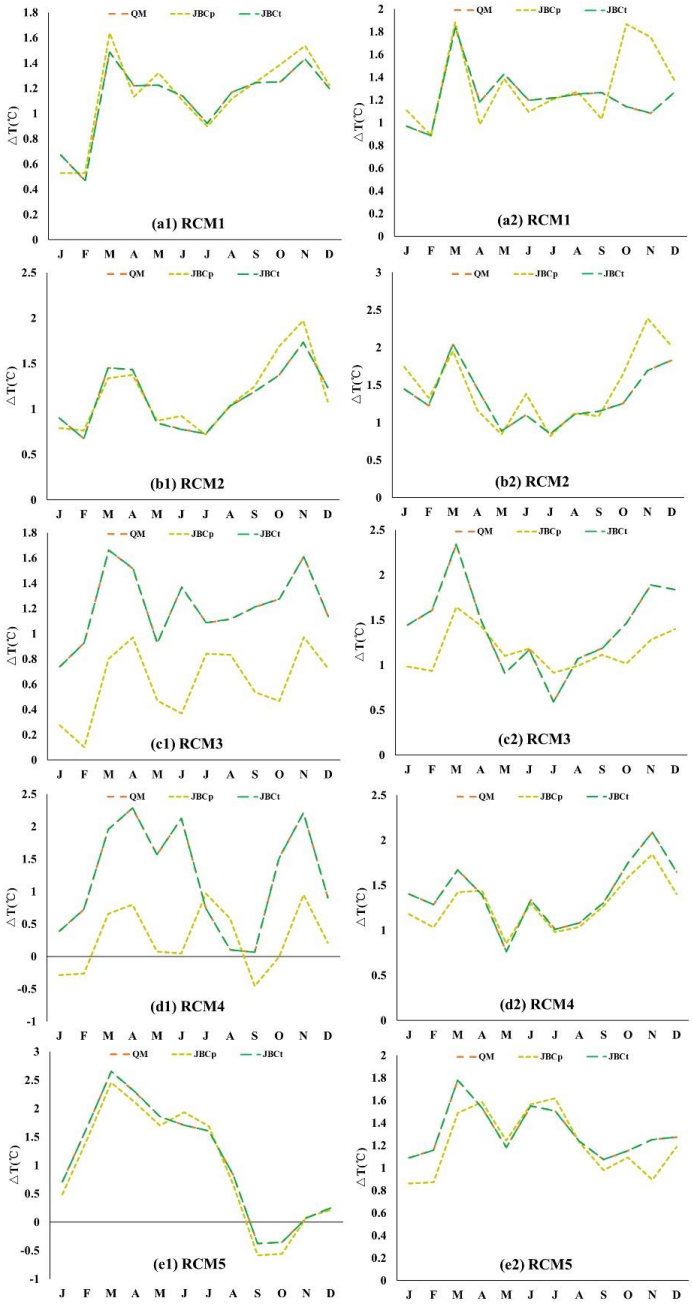

620

621 Figure 9. Change of basin-wide temperature in the future period projected by corrected RCMs under

622 RCP4.5 (left column) and RCP8.5 (right column) scenarios compared to the historical period.

623

Hydrol. Earth Syst. Sci. Discuss., https://doi.org/10.5194/hess-2018-251
Manuscript under review for journal Hydrol. Earth Syst. Sci.
Discussion started: 14 May 2018

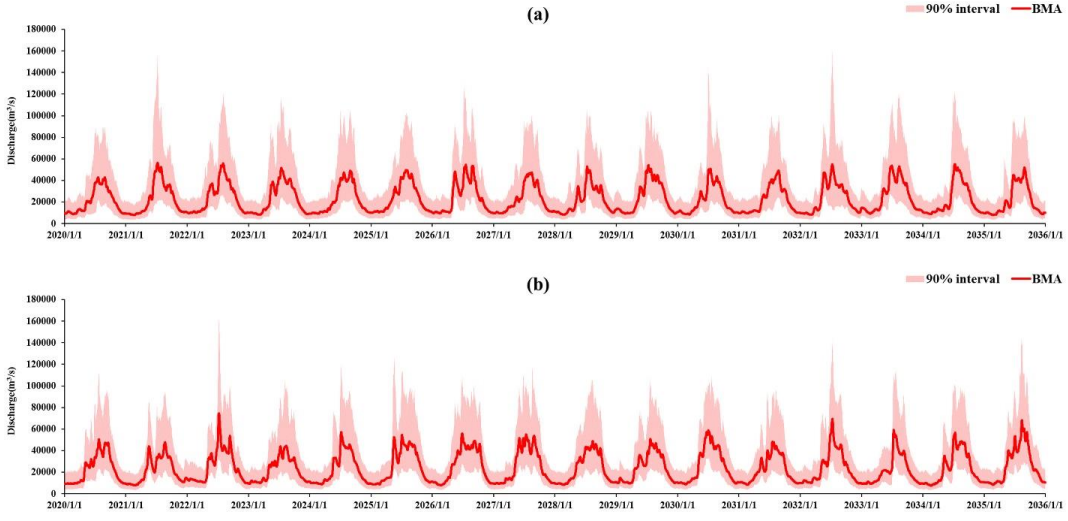

Figure 10. The mean values and 90% uncertainty interval of streamflow simulated by the BMA method during the future period under (a) RCP4.5, (b) RCP8.5 scenarios at Bahadurabad.

Hydrol. Earth Syst. Sci. Discuss., https://doi.org/10.5194/hess-2018-251
Manuscript under review for journal Hydrol. Earth Syst. Sci.
Discussion started: 14 May 2018

Hydrology and Earth System Sciences
Open Access
Discussions

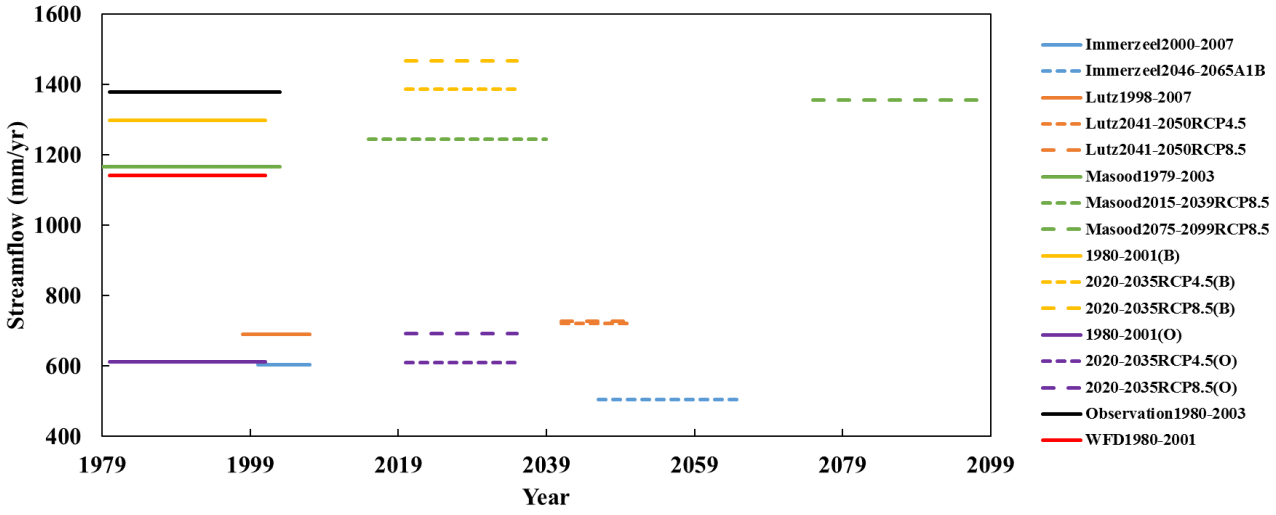

628
629 Figure 11. Streamflow projections from the existing studies during different periods at different locations (B denotes Bahadurabad in the
630 downstream, O denotes the upper YBR basin outlet, see Figure 1 for the location).